

Research

Environmentally-induced noise dampens and reddens with increasing trophic level in a complex food web

Anna Kuparinen, Tommi Perälä, Neo D. Martinez and Fernanda S. Valdovinos

A. Kuparinen (http://orcid.org/0000-0002-7807-8946) (anna.k.kuparinen@jyu.fi) and T. Perälä, Dept of Biological and Environmental Science, PO Box 35, FI-40015 University of Jyväskylä, Finland. – N. D. Martinez, Dept of Ecology and Evolutionary Biology, Univ. of Arizona, Tucson, AZ, USA. – F. S. Valdovinos, Dept of Ecology and Evolutionary Biology, Univ. of Michigan, Ann Arbor, MI, USA, and: Center for the Study of Complex Systems, Univ. of Michigan, Ann Arbor, MI, USA.

Oikos

00: 1–13, 2018 doi: 10.1111/oik.05575

Subject Editor: Yngvild Vindenes Editor-in-Chief: Dustin Marshall Accepted 17 October 2018 Stochastic variability of key abiotic factors including temperature, precipitation and the availability of light and nutrients greatly influences species' ecological function and evolutionary fate. Despite such influence, ecologists have typically ignored the effect of abiotic stochasticity on the structure and dynamics of ecological networks. Here we help to fill that gap by advancing the theory of how abiotic stochasticity, in the form of environmental noise, affects the population dynamics of species within food webs. We do this by analysing an allometric trophic network model of Lake Constance subjected to positive (red), negative (blue), and non-autocorrelated (white) abiotic temporal variability (noise) introduced into the carrying capacity of basal species. We found that, irrespective of the colour of the introduced noise, the temporal variability of the species biomass within the network both reddens (i.e. its positive autocorrelation increases) and dampens (i.e. the magnitude of variation decreases) as the environmental noise is propagated through the food web by its feeding interactions from the bottom to the top. The reddening reflects a buffering of the noise-induced population variability by complex food web dynamics such that non-autocorrelated oscillations of noise-free deterministic dynamics become positively autocorrelated. Our research helps explain frequently observed red variability of natural populations by suggesting that ecological processing of environmental noise through food webs with a range of species' body sizes reddens population variability in nature.

Keywords: coloured noise, ecosystem dynamics, environmental stochasticity

Introduction

Interactions between environmental variation and biological systems are key concerns within ecology, evolutionary biology, and in the management of many species' populations. These concerns are becoming increasingly relevant due to the rapid changes in the abiotic environment caused by humans that are altering the structure and dynamics of populations and ecosystems (Walther et al. 2002, Ceballos et al. 2017). More specifically, temporal variation in temperature, precipitation, and the availability of light and nutrients can produce species extinctions, pest outbreaks,



www.oikosjournal.org

© 2018 The Authors. Oikos © 2018 Nordic Society Oikos

and dramatic changes in the composition of communities. Despite the centrality and urgency of these concerns, theory about how complex biological communities respond to stochastic variation in their abiotic environment focuses almost entirely on the dynamics of one or a few interacting species (Kaitala et al. 1997, Ripa et al. 1998, Ruokolainen et al. 2009a). Here, we extend such theory (Ripa et al. 1998) by analysing how environmental stochasticity propagates within a well-studied complex food web.

In addition to the magnitude of variability, time series of environmental variables and population abundances often exhibit a distinct temporal structure (Halley 1996) that is characterized in terms of the colour of temporal variability often referred to as 'noise' (Ruokolainen et al. 2009a). Red noise characterizes the slow change of variables whose consecutive values in a time series are relatively similar, that is, their fluctuations are positively auto-correlated. Conversely, blue noise characterizes the rapid change of variables (e.g. from high to low values) whose fluctuations are negatively auto-correlated. Finally, white noise characterizes variables that are temporally uncorrelated (for empirical examples, Ruokolainen et al. 2009a). Natural fluctuations of environmental variables (Vasseur and Yodzis 2004) and population abundances (Pimm and Redfearn 1988, Cohen 1995, Sugihara 1995, Burgers 1999) tend to be red coloured, with marine variables more red than terrestrial ones (Vasseur and Yodzis 2004), with the noticeable exception of El Niño southern oscillation which is characterized by blue noise (Burgers 1999). Nonetheless, theory about deterministic population dynamics have not managed to capture the mechanisms that lead to red-coloured variations. Cohen (1995) showed that chaotic dynamics of a range of commonly applied deterministic single-population models tend to be blue. Cohen (1995) concluded that 'It is not yet known whether this dilemma can be resolved by expanding the models to take account of environmental fluctuations, the interactions of single species with other species, or the age structure and spatial distribution of populations.'

Indeed, incorporation of coloured environmental noise into single-species population dynamics models has demonstrated that population variability reflects the interaction between environmental noise and demography. Population fluctuations resulting from such interactions can be of virtually any colour, depending on population stability, growth rate, and the extent to which population dynamics are chaotic (Sugihara 1995, Kaitala et al. 1997). It thus remains unsolved, which mechanism present across a broad range of natural populations is responsible for the reddening (i.e. population variation tending to be positively autocorrelated irrespective of the colour of environmental noise they are affected by). Kaitala et al. (1997) detected an association of increased complexity of single-species dynamics with increased reddening, suggesting that oversimplified population models might be responsible for the mismatch between theory and observations (reviewed in the previous paragraph). Indeed, analyses of simple two-species food webs demonstrate that

species interactions markedly complicate the ways in which environmental variability manifests in population dynamics (Ripa et al. 1998). Ripa et al. (1998) found conditions for food webs of predators and prevs interacting via linear functional responses where the species not subjected to environmental noise generally express redder (i.e. more positively autocorrelated) variation than the species subjected to noise. However, these conditions regarding the value of Jacobian matrices and the restriction to linear interactions limit the generality of this finding, especially with respect to more realistically complex food webs with nonlinear interactions and populations structured according to life history (Mougi 2017). Here, we study a food web with these complexities to explore how coloured environmental noise (Ripa et al. 1998, Fig. 1) combined with changing magnitudes of environmental variability (Ruokolainen et al. 2009a), may alter the dynamics of populations and the ecosystem.

Allometric trophic network (ATN) theory has substantially improved ecologists' abilities to understand and predict complex food web dynamics (Brose et al. 2006, Berlow et al. 2009, Boit et al. 2012), by basing the rates of consumerresource interactions on the straight-forward and empirically well-founded allometric scaling with body size (Brose et al. 2006). For example, an ATN model of the Lake Constance (Alpine lake in central Europe; hereafter LC) explained up to 82% of variability in seasonal dynamics of 24 species within the lake's complex food web (Boit et al. 2012). Based on this success, we use the LC ATN model as an empirically corroborated template to study food-web dynamics. More specifically, we use a version of the LC ATN model that includes the age-structured dynamics of fishes (Kuparinen et al. 2016) to study how environmental noise introduced into basal production filters through the food web and manifests at different trophic levels up to fishes at the top of the food web. The complexities of age-structured fish populations and nonlinear interactions within our LC ATN model make it impossible to predict our model's population colour spectra based on previously published theory (V. Kaitala pers. comm.).

Material and methods

Deterministic ATN model for Lake Constance (LC) food web dynamics

The LC ATN model is an allometric trophic network model of the lake's food web dynamics developed and parameterized by Boit et al. (2012) and modified by Kuparinen et al. (2016) to better address the life-history structure of fishes. The modelled network contains 133 feeding links among 30 functionally distinct guilds of which six are basal producers, seven are heterotrophic microbes, seven are invertebrates, and 10 are five life-history stages (larvae, juveniles, 2 years, 3 years, and 4 years and older hereafter denoted as 4+) of two species of fish (perch and whitefish, Fig. 2, Supplementary material Appendix 1 Table A1).

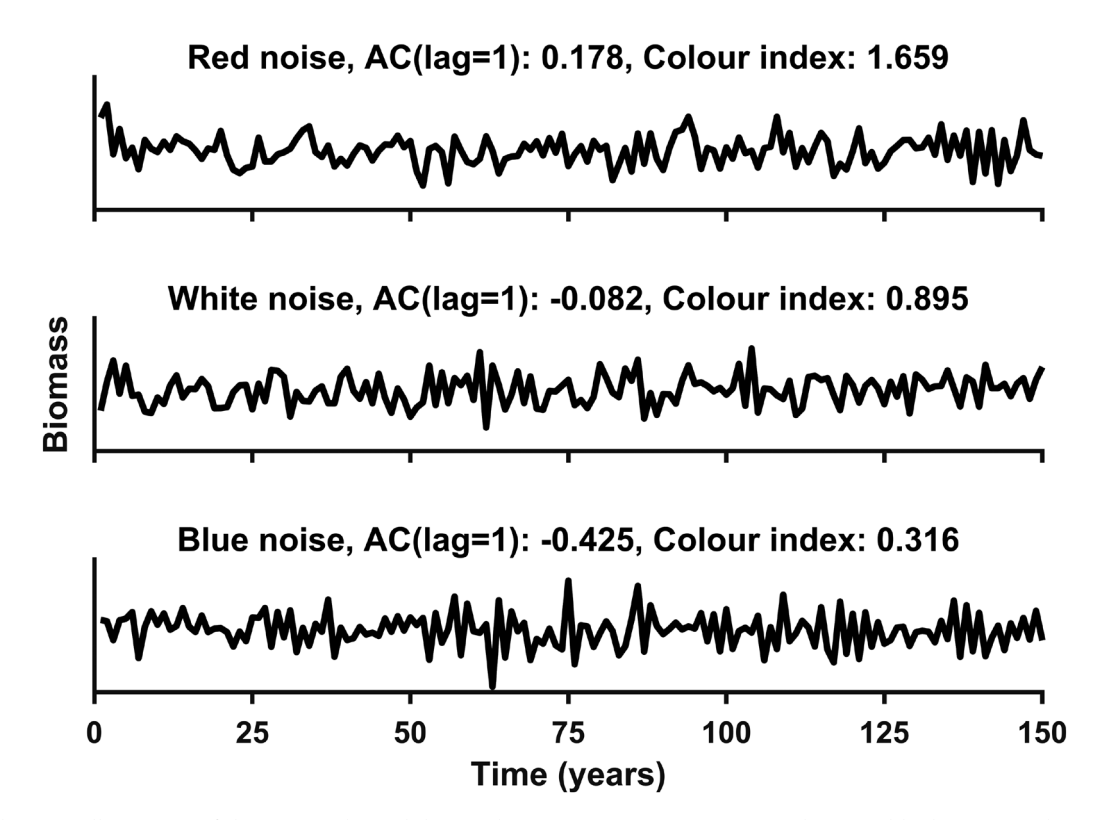


Figure 1. Schematic illustration of the temporal variability in the most common primary producer guild when exposed to red, white and blue noise (autocorrelation 0.4, 0 and -0.4 respectively; SD is 15% of K_0). The guild is filamentous blue and green algae (Alg3, Supplementary material Appendix 1). Each panel also show the lag 1 autocorrelation and the colour index for the temporal variability of the guild biomass abundance.

The dynamics of the system are divided into two parts. In the first part, the food web dynamics for year Y are simulated in continuous time during the 'growth season'. This part includes the producer growth, consumer and fish feeding, maintenance of organism's bodily functions, and the allocation of portion of adult fish biomass for reproduction. These dynamics are modelled as a system of ordinary differential equations (ODEs). The second part of the system dynamics is called 'reproduction and aging' and it consists of the birth of new fish larvae and the transfer of fish biomass to the next life stage for year Y+1.

Growth season dynamics

The core biomass dynamics of species or groups of functionally similar species (i.e. guilds, denoted by their index i; Supplementary material Appendix 1 for detailed guild information) within the growth season of year Y are described by a set of ordinary differential equations. The biomass of guild i and its derivative with respect to time are denoted by $B_{Y,i}(t)$ and $\dot{B}_{Y,i}(t)$, respectively, where $t \in [t^{\text{init}}, t^{\text{end}}]$. The vector of all guild biomasses is denoted by $B_{Y}(t)$. The length of the growth season is 90 days, and thus we set $t^{\text{init}} = 0$ and $t^{\text{end}} = 90$. For notational simplicity, we omit the year Y and time t from the description of the growth season dynamics.

Producer guild ($i \in \{1, ..., 6\}$) dynamics are driven by their intrinsic (logistic) growth and the feeding subjected to them

by their herbivore predators. The ODE for the biomass of producer guild i during the growth season is

$$\dot{B}_{i} = \overbrace{r_{i}B_{i}G_{i}(B)(1-s_{i})}^{\text{gain from producer growth}} - \sum_{j} \underbrace{\frac{\sum_{j} y_{ji}B_{j}F_{ji}(B)}{x_{j}y_{ji}B_{j}F_{ji}(B)}}_{e_{ji}}$$
(1)

where r_i is the mass-specific intrinsic growth rate of producer i (Boit et al. 2012); $G_i(\mathbf{B}) = 1 - \left(\sum_{j=\text{producers}} c_{ij} B_j\right) / K$ is the limiting factor in the logistic growth model of the producers, and it includes producer competition coefficients c_{ij} and carrying capacity coefficient K shared by all autotrophs; s_i is the fraction of exudation; x_i is the mass-specific metabolic rate of consumer i based on allometric scaling; y_{ij} is the maximum consumption rate of guild i feeding on guild j; e_{ji} is the assimilation efficiency describing the fraction of ingested biomass lost by egestion. $F_{ji}(B)$ is the functional response (see below).

Consumer guild (including bacterial detritivores; $i \in \{7, ..., 20\}$) dynamics consists of the maintenance of bodily functions, gains from feeding on their prey, and losses due to getting fed on by their predators, and the ODE is

$$\dot{B}_{i} = -\int_{f_{m}}^{\text{maintenaceloss}} + \int_{a}^{\text{gainfrom resources}(j)} + \int_{a}^{\text{loss to consumer } j} \frac{1}{x_{j} y_{ji} B_{j} F_{ji}(\mathbf{B})} - \sum_{j} \frac{1}{x_{j} y_{ji} B_{j} F_{ji}(\mathbf{B})}$$
(2)

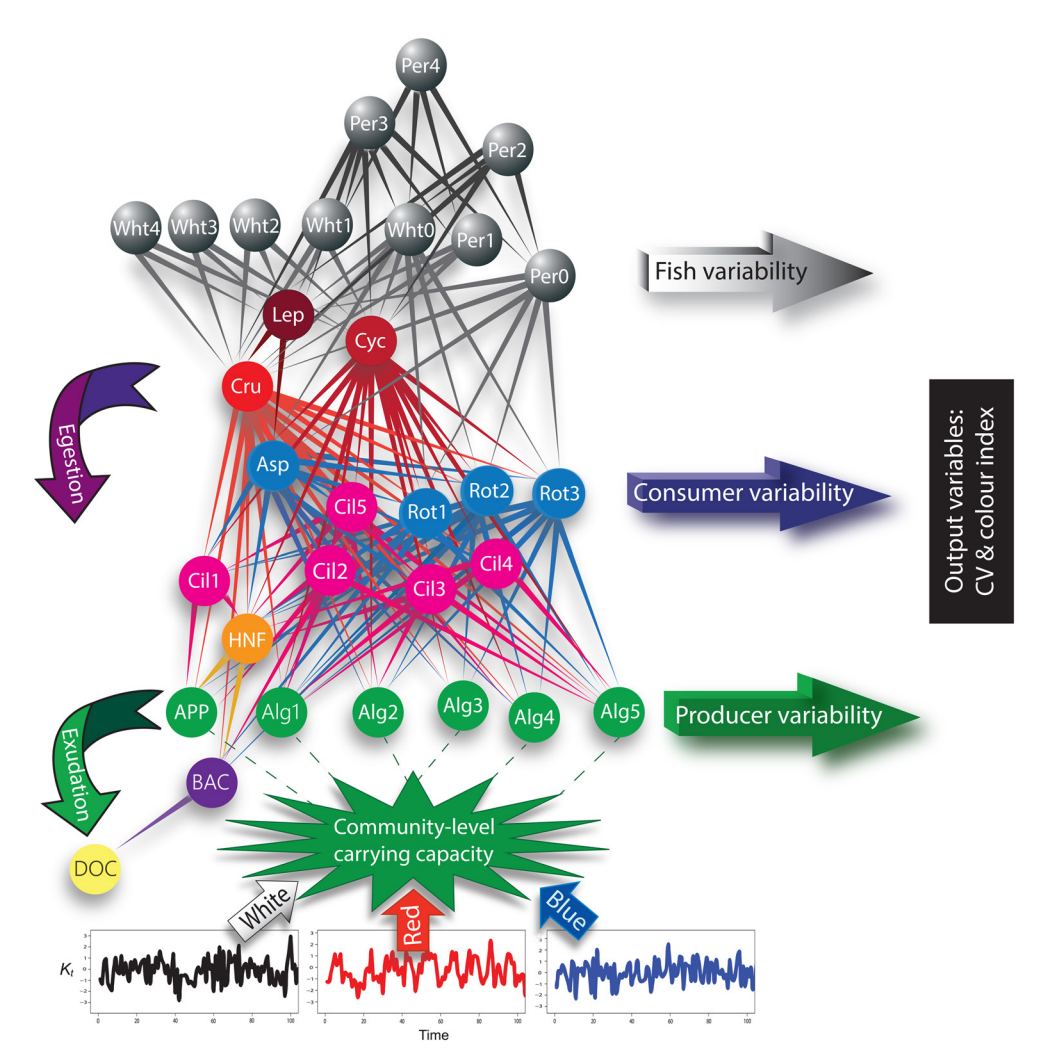


Figure 2. A schematic illustration of the analysis of the effects of environmental noise on the Lake Constance food web dynamics. Each spherical node represents one of the 30 trophic groups. Trophic groups were aggregated into three functional groups for certain analyses. Producers include all the algae guilds (Alg1–Alg5) and the autotrophic picoplankton guild (APP) at the bottom of the food web. Consumers include all other trophic groups such as ciliates (Cil1–Cil5), rotifers (Rot1–Rot3) and Daphnia (Dap). Fishes include all the age classes of the Whitefish (Wht0–Wht4) and Perch (Per0–Per4). Dissolved organic carbon (DOC) is supplied by heterotrophic egestion and autotrophic exudation and is consumed by bacteria (Bac). Guild labels and colours are further explained in Supplementary material Appendix 1 Table A1. Links represent energetic pathways from guilds at the pointed end to guilds on the thicker end. In the simulations of the food web dynamics, differing magnitudes and colours of environmental noise is introduced into the phytoplankton community carrying capacity (K_i). The impacts of the environmental noise on each individual guild and aggregated functional groups is then investigated by analysing the coefficient of variation (CV) and the colour index of the time series of their biomasses.

where f_m is the fraction of assimilated carbon respired by maintenance of basic body functions; and f_a is the fraction of assimilated carbon used for production of consumers' biomass under activity $(1-f_a$ is respired). $F_{ij}(\mathbf{B})$ is the consumer and fish species' normalized functional response to prey species densities

$$F_{ij}(\mathbf{B}) = \frac{\omega_{ij}B_j^q}{B0_{ij}^q + d_{ij}B_iB0_{ij}^q + \sum_{l=\text{resources}}\omega_{il}B_l^q}$$
(3)

where ω_{ij} is the relative prey preference of consumer species i feeding on resource species j; q = 1.2 which

forms a relatively stable version of the Holling type-II functional response (Williams and Martinez 2008); $B0_{ij}$ is the half saturation constant of resource species j at which consumer species i achieves half of its maximum feeding rate on species j; d_{ij} is the coefficient of intraspecific feeding interference of species i while feeding on species j. The parameter d_{ij} also accounts for prey resistance to consumption.

The fish guilds have indices 21-30 so that whitefish have odd and perch have even indices. The growth season dynamics of the larval and juvenile fish guilds ($i \in \{21, ..., 24\}$) are identical to the consumers' dynamics, i.e.

$$\dot{B}_{i} = -f_{m}x_{i}B_{i} + f_{a}x_{i}B_{i}\Sigma_{j}y_{ij}F_{ij}\left(\boldsymbol{B}\right) - \Sigma_{j}\frac{x_{j}y_{ji}B_{j}F_{ji}\left(\boldsymbol{B}\right)}{e_{ii}}$$
(4)

The adult fish guilds ($i \in \{25, ..., 30\}$) have no predators in our model and they allocate a portion of the surplus biomass from growth to reproduction (only if there is surplus, i.e. gains from feeding are greater than the maintenance costs). The ODE modelling the biomass of adult fish guild i can, thus, be written as

$$B_{Y+1,i}(t^{\text{init}}) = B_{Y,i-2}(t^{\text{end}}), \quad i \in \{23,...,28\}.$$
 (9)

The oldest life stage (age 4+) consists of the 4-year old fish and all the older fish, and thus the initial biomass of the 4+ group for year Y+1 is a sum of the 4+ and 3 group biomasses at the end of the growth season of year Y,

$$B_{Y+1,i}(t^{\text{init}}) = B_{Y,i}(t^{\text{end}}) + B_{Y,i-2}(t^{\text{end}}), i \in \{29,30\}.$$
 (10)

$$\dot{B}_{i} = \begin{cases} -f_{m}x_{i}B_{i} + f_{a}x_{i}B_{i}\Sigma_{j}y_{ij}F_{ij}(\boldsymbol{B}), & f_{m}x_{i}B_{i} \geq f_{a}x_{i}B_{i}\Sigma_{j}y_{ij}F_{ij}(\boldsymbol{B}) \\ (1 - P_{i}I_{i})(-f_{m}x_{i}B_{i} + f_{a}x_{i}B_{i}\Sigma_{j}y_{ij}F_{ij}(\boldsymbol{B})), & f_{m}x_{i}B_{i} < f_{a}x_{i}B_{i}\Sigma_{j}y_{ij}F_{ij}(\boldsymbol{B}) \end{cases}$$

$$(5)$$

Here P_i denotes the proportion of mature biomass in adult fish guild i, and I_i denotes the fraction of the mature surplus biomass that is invested into reproduction. The biomass allocated to reproduction is not available for growth and is thus considered in (5). We use \dot{B}_i^+ to denote the rate of biomass allocation to reproduction by adult fish guild i during the growth season, and add

$$\dot{B}_{i}^{+} = P_{i}I_{i} \cdot \max\left(0, -f_{m}x_{i}B_{i} + f_{a}x_{i}B_{i}\Sigma_{j}y_{ij}F_{ij}\left(\boldsymbol{B}\right)\right),$$

$$i \in \left\{25, \dots, 30\right\}$$
(6)

to the system of ODEs.

The detritus (i=0) dynamics consists of the egestion caused by feeding, producer exudation, and loss to consumption by detritivores (bacteria):

Parameterization for Lake Constance food web

The ATN model parameterization for Lake Constance food web utilized in the present study was first developed and validated by Boit et al. (2012) and then further extended by Kuparinen et al. (2016) to account for fish life-history dynamics. Functional guilds, i.e. nodes in the food web, along with their feeding links and guild properties are given in Supplementary material Appendix 1 Table A1. Among producers, interspecific competition $(c_{ij}, i \neq j)$ was set to 1 and intraspecific producer competition $(c_{ij}, i = j)$ was set to a value (2.0225) that creates (Chesson and Kuang 2008) deterministic dynamics of the producers, consumers and fishes with white-coloured oscillations about the equilibrium, which

$$\dot{B}_{0} = \sum_{i} \left[\sum_{j} \frac{x_{i} y_{ij} B_{i} F_{ij}(B)}{e_{ij}} \underbrace{(1 - e_{ij})}_{\text{egestion}} \right] + \sum_{i} \underbrace{r_{i} B_{i} G_{i}(B) s_{i}}_{\text{excudation by producer } i} - \sum_{j} \underbrace{x_{j} y_{ji} B_{j} F_{ji}(B)}_{e_{ji}}$$

$$(7)$$

The simulation starts at year Y=1, and the initial biomass vector $\boldsymbol{B}_1(t^{\text{init}})$ consists of the biomasses at the system's equilibrium and the initial value for $B_{Y,i}^+=0, \forall i\in\{25,...,30\}, \forall Y$. The system of ODEs is then solved for the growth season.

Reproduction and aging

After the growth season of year Y, the accumulated biomass allocated to reproduction $B_{Y,i}^+(t^{\rm end})$ by the adult fish guild i translates to initial larvae biomass for the next year's growth season. The initial biomass of the larvae for year Y+1 for a given fish species is the sum of the larvae produced by the different adult life-stages of that fish species, i.e.

$$B_{Y+1,i}(t^{\text{init}}) = \sum_{a=2}^{4} B_{Y,i+2a}^{+}(t^{\text{end}}), \quad i \in \{21,22\}.$$
 (8)

The initial biomasses of the juveniles (age 1), and the two first adult life stages (ages 2 and 3) for year Y+1 are the biomasses of the previous life stages at the end of the growth season of year Y,

facilitates analyzing the effects of environmental noise on our model's dynamics. Table 1 for other parameter values.

Environmental noise scenarios

Our objective was to explore how environmental noise propagates through the food web from its bottom to the top of the food web and interacts with species properties. To this end, we introduced annually (i.e. for each growth season) environmental noise into the producers' community-level carrying capacity, K. We did this by calculating K for year t as: $K_t = (1 - \kappa) K_0 + \kappa K_{t-1} + v_t$, where K_0 estimates Lake Constance's long-term carrying capacity for primary producers (Supplementary material Appendix 1) as 540 000 μ g C m⁻³ (Boit et al. 2012, Kuparinen et al. 2016), $|\kappa| < 1$ is the autocorrelation between K_t and K_{t-1} , and $V_t \sim N\left(0,\sigma^2\left(1-\kappa^2\right)\right)$ is a normally distributed random variable. The expected value $E(K_t) = K_0$ and the standard deviation $SD(K_t) = \sigma$ for all t (Ruokolainen et al. 2009). K_t is restricted to be positive by rejecting sampled value if it is

Table 1. Summary of the ATN model parameters for Lake Constance. Adapted from Kuparinen et al. (2016).

Parameter	Unit	Value	Description	Reference	
K	μgC m ⁻³	540 000	phytoplankton carrying capacity	Boit et al. (2012)	
X_i	day ⁻¹	0.04-0.18	mass-specific metabolic rate ¹	Brose et al. (2006)	
r_i	day ⁻¹	0.6-1.09	mass-specific growth rate for autotrophs ¹	Brose et al. (2006)	
C _{ii}	,	1 (2.0225 for $i=j$)	producer competition coefficient	Boit et al. (2012)	
$f_{a}^{"}$		0.4	activity metabolism coefficient	Humphreys (1979)	
f_m		0.1	maintenance respiration coefficient	Humphreys (1979)	
 Y _{ij}		10	maximum ingestion rate	Yodzis and Innes (1992), Brose et al. (2006)	
e_{ii}		0.66	assimilation efficiency	Nielsen and Olsen (1989)	
d_{ii}	$m^3 \mu g C^{-1}$	0-0.5	feeding interference coefficient	Skalski and Gilliam (2001), Boit et al. (2012)	
$q^{''}$		1.2	functional response shape parameter	Boit et al. (2012)	
ω_{ii}		0-0.5	relative prey preference	Boit et al. (2012)	
p_{ii}		0–1	fraction of resource species shared	Boit et al. (2012)	
S_i		0.2	fraction of exudation	Boit et al. (2012)	
BO_{ij}	$\mu g C m^{-3}$	1500-700 000	half-saturation densities	Boit et al. (2012)	

¹Relative rates with respect to guild 1; Supplementary material Appendix 1 Table A1.

non-positive. Environmental noise scenarios are characterized by the magnitude (SD) and 'colour' (autocorrelation, κ) of variation in K_{τ} (Ruokolainen et al. 2009a; Fig. 1). We set $SD(K_{\tau})$ to 5%, 10%, 15% or 20% of K_{0} . We set κ to 0 for white (uncorrelated) noise, 0.4 for red (positively autocorrelated) noise, and -0.4 for blue (negatively autocorrelated) noise.

Simulation design and output variables

Initial biomasses for each guild emerged from simulating 150 years (growth seasons) of deterministic model dynamics with the (noise-free) constant K_t set to K_0 . We discarded the first 50 'burn-in' years during which the guilds settled into their dynamic equilibrium that we analysed during the following 100 years. Each simulation scenario was replicated for 100 times (larger number of replicates gave analogous results).

We focus on investigating how the different environmental noise scenarios affect the magnitude and the nature of variability in the guild biomass within the food web (Fig. 2), and how such variability may be explained by the properties of the guild. Throughout these analyses, biomasses at the end of each growth season, after the production of new larvae, is the central response variable. This limits our shortest observation scale to the scale at which variability is introduced to the system and thus avoids biasing our results with trivial positive correlations between subsequent time steps within a growth season. We quantify the magnitude of the year-to-year variability through the coefficient of variation (CV) across the last 100 years of each simulation, estimated by dividing the sample SD with the sample average. We estimated the colour of the variability using a colour index of the time series of each guild's biomass (Blarer and Doebeli 1996). This colour index integrates across relative contributions of low and high frequency fluctuations across the time series. Dominance of low or high frequency fluctuations corresponds to red or blue noise and to positive or negative autocorrelation, respectively. White noise occurs when the spectrum is relatively evenly

distributed across all frequencies (Blarer and Doebeli 1996, Kaitala et al. 1997, Ripa et al. 1998). We calculated the raw power spectrum (using spec function in R, which produces frequency spectrum for a time series; <www.r-project.org>) for each replicated run across a 100-year time period and divided the average of the spectral values for frequencies 0–0.25 by the average of the spectral values for frequencies 0.25–0.5. Values above 1, close to 1, or below 1 indicate red, white, or blue noise, respectively. In addition to the colour index integrating over the lags in temporal autocorrelation, we also estimated simple autocorrelation coefficients for lag = 1 (i.e. AR(1)), which are commonly utilized to explore the colour of variation in environmental time series (Ruokolainen et al. 2009a).

Guild covariates and statistical analyses

We analysed the temporal variation in the biomasses of the guild both separately and also grouped into producers, nonfish consumers (hereafter just 'consumers'), or fishes. Due to skewness, the colour index values were log-transformed. The magnitude (CV) and the log-transformed colour index were explored through ANOVAs, with the autocorrelation κ of the input noise, SD and species type, and their interactions as explanatory variables. Differences in the log-transformed average colour index values between the species types were further investigated through *t*-tests. We explored whether the magnitude (CV) and the colour index of biomass variations of individual guilds can be explained by the guild properties. These properties include the natural logarithm of their body size; guild's connectivity defined by the number of guilds it is connected to (as a predator or a prey) standardized by $2 \times L/S$, where L is the total number of links in the food web and S is the total number of guilds; and their short-weighted trophic level (Williams and Martinez 2008, Carscallen et al. 2012). The effects of these covariates were explored through linear models explaining the magnitude (CV) and the logtransformed colour index (responses) of biomass variability (response variables) with SD, κ , and their interaction as well

as each of the guild's covariates separately (due to collinearity among the covariates) as explanatory variables. Normality of the residuals was explored through qq-plots.

Data deposition

Data available from the Dryad Digital Repository: http://dx.doi.org/10.5061/dryad.75mg6b1 (Kuparinen et al. 2018). Data and codes used in this manuscript are included in the Supplementary material Appendix 1.

Results

In the fully deterministic 'baseline' scenario, where no noise was introduced into K_i , the temporal variability in the biomass of producers, consumers and fishes showed similar year-to-year variation reflecting the deterministic oscillations (wave length of 4 years) emerging from the food web dynamics (Fig. 3). In the stochastic scenarios, where noise

was introduced into K_p , the biomass variability (as reflected in the CVs) generally increased most prominently at low trophic levels. Producers and fishes displayed the largest and smallest variation, respectively, at each noise magnitude and colour scenario. In all cases, the food web consistently dampens (i.e. reduces) the variation as the trophic level increases, as is seen in the decreasing vertical positions and in the heights of the CV boxplots in Fig. 3. Within producers, consumers and fishes, increasing the noise magnitude (SD) resulted in increased biomass variability, whereas changing the noise colour had little effect on the amount of biomass variability (Fig. 3).

Introduction of noise into K_t caused this variability to differentiate, such that the colour index values were reddened with increasing trophic level or, in other words, the colour index systematically increases as one goes from producers through consumers to fishes (Fig. 4). Producers' temporal biomass variability closely mirrored the variability introduced into K_t , such that white noise led to producer colour index values close to one, red noise to values larger than one, and

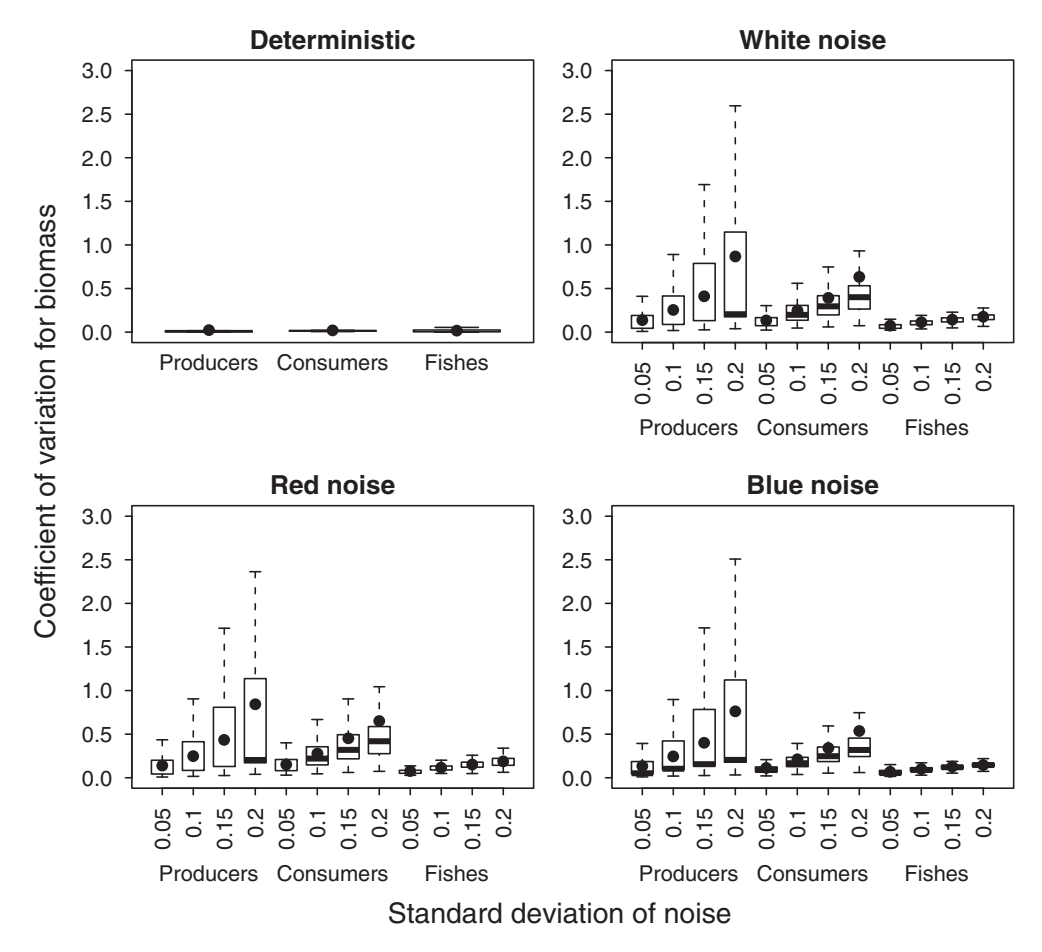


Figure 3. Coefficients of variation (CV) for the biomasses of producers, consumers, and fishes under alternative noise scenarios. The standard deviations of normally distributed noise introduced into the phytoplankton carrying capacity are indicated on the x-axis (0.05–0.2) and the noise colour scenarios as well as deterministic food web dynamics in the absence of noise are shown in separate panels. Medians are indicated by horizontal lines, boxes span the inter-quartile range, and whiskers encompass values 1.5 box lengths away from the box. Averages are plotted with black bullets. Outliers are not shown.

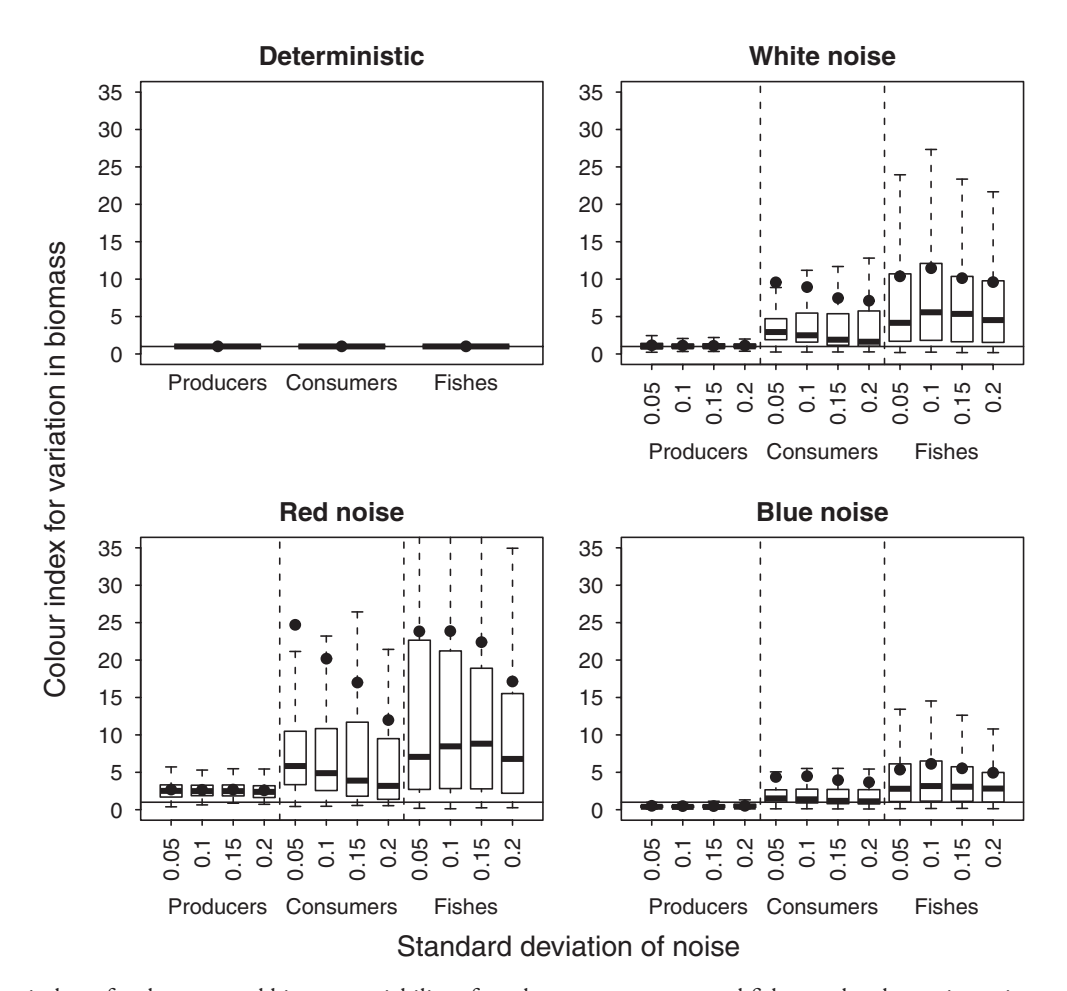


Figure 4. Colour indexes for the temporal biomass variability of producers, consumers, and fishes under alternative noise scenarios. Colour index values below one (horizontal line) indicate blue (negatively autocorrelated) variation, values above one red (positively autocorrelated) variation, and values close to 1 indicate white (non-autocorrelated) variation. Other figure elements are the same as in Fig. 3. The distributions of the colour index values were highly skewed, which is reflected in the discrepancy between the averages and the medians, the latter being generally more robust with respect to outliers than the former.

blue noise to values lower than one, indicative of white, red, and blue variability, respectively. In contrast, the temporal biomass variability of consumers and fishes was red (colour index values above one) irrespective of the colour of the noise introduced into K. Still, the shades of this red variability shifted from the least to the most red as the colour of the noise introduced into the producer carrying capacity shifted from blue through white to red. Increasing the magnitude of the noise (SD) typically reduced the amount of reddening of the variability of producers, consumers and fishes (Fig. 4). Variability measured by autocorrelations at lag = 1 showed similar results: the variability of consumers and fishes was always redder (positive autocorrelation), whereas the colour of the producers' variability more closely reflected the colour of the noise introduced into K_t (Supplementary material Appendix 1 Fig. A1).

Analyses of variance of the magnitude (CV) and the logtransformed colour index of biomass variability largely confirmed the patterns detected visually. Most of the variation in CV was associated with the SD of the noise introduced into K, species type, and their two-way interaction, whereas the colour of the noise had negligible effects (Table 2). The variation in the colour index values was largely attributable to the effects of the colour of the noise and species type whereas SD had an order-of-magnitude lower effect (Table 2). To confirm that the variation of consumer and fish biomasses is red irrespective of the colour of the noise introduced into K, one-way t-tests were performed to compare the log-transformed colour index values with the threshold value 0 (log of 1). Across all the simulation scenarios, the log-transformed colour index was significantly larger than 0 for both the consumers (mean: 1.34, 95% CI: 1.32-1.36, t-value: 115.84, df: 16799, p<0.001) and the fishes (mean: 1.73, 95% CI: 1.71–1.76, t-value: 129.66, df: 11999, p < 0.001). Similarly, log-transformed colour indexes were significantly higher among fishes than among consumers (t-value: 22.205, df: 26210, p < 0.001).

The analyses of the guild covariates reflected the patterns seen in Fig. 3, 4. In general, low *CV*s and high colour index values were associated with large body size (and, thus, high

Table 2. Analyses of variances of the biomass coefficient of variation (CV) and the log-transformed colour index for biomass variation as responses, explained by the magnitude (SD) and colour (white, red, blue) of the environmental noise and species type (producer, consumer, fish).

Resp.	Variable	df	Sum Sq	Mean Sq	F-value	p-value
Biomass CV	colour	2	17.2	8.62	33.9	2.034e-15
	SD	1	747.7	747.7	2936.7	<2.2e-16
	species type	2	479.8	239.9	942.3	<2.2e-16
	colour×noise	2	4.1	2.07	8.13	2.951e-4
	colour×species type	4	5.1	1.27	4.99	5.131e-4
	<i>SD</i> ×types	2	235.6	117.79	462.7	<2.2e-16
	colour $\times SD \times sp.$ type	4	0.7	0.17	0.6739	0.6100
	residuals	36 012	9168.4	0.25	_	_
log(colour index)	colour	2	9368	4683.8	3458.5	<2.2e-16
O	SD	1	193	193.3	142.7	<2.2e-16
	species types	2	10 845	5422.7	4004.1	<2.2e-16
	colour×noise	2	29	14.6	10.75	2.141e-5
	colour×species type	4	403	100.6	74.31	<2.2e-16
	<i>SD</i> ×types	2	127	63.6	46.94	<2.2e-16
	colour $\times SD \times sp.$ type	4	15	3.7	2.74	0.02693
	residuals	35 982	48 730	1.4	_	_

trophic level as these two variables are strongly correlated; Fig. 5, 6). In the linear models, the log-transformed body mass performed best in explaining the variation in CV. The proportions of variation (R²) in CV explained by the models with log-transformed body mass, trophic level, and connectivity as covariates were 14.3%, 11.2% and 10.1%, respectively, whereas R² for a model without guild covariates was 7.8%. For the log-transformed colour index, trophic level slightly outperformed log-transformed body mass and connectivity had virtually no effect (R²'s were 33.8%, 27.7% and 15.8% for models with trophic level, log-transformed body mass and connectivity, respectively, and 15.4% for the model without guild covariates).

Given that the environmental noise induced to the *K* can affect producers with differing growth rates differently, we explored the robustness of our results by implementing noise directly to producer growth dynamics through

$$\dot{B}_{i} = \overbrace{(r_{i}B_{i}G_{i}(\boldsymbol{B}) + B_{i}\varepsilon)(1 - s_{i})}^{\text{gain from producer growth}} - \Sigma_{j} \underbrace{\frac{x_{j}y_{ji}B_{j}F_{ji}(\boldsymbol{B})}{e_{ji}}}_{\text{loss to consumer } j}$$

$$(11)$$

where ε is the environmental noise term. Otherwise, the simulation design was the same. This alternative method produced results analogous to those presented above (Supplementary material Appendix 1 Fig. A2, A3), thus confirming the robustness of our results to the way in which noise was introduced to the bottom of the food web.

Discussion

The present study demonstrates how environmental noise introduced at the basal level of a food web both reddens and dampens as it is propagated from the bottom to the top of the food web by species' feeding interactions. We introduce

noise at the bottom level of the food web because environmental stochasticity can be expected to more acutely impact autotrophs' critical resources such as light and nutrient availability than the intrinsic growth rates of the species or heterotrophs' critical resources such as prey species' abundances. Additionally, altering the intrinsic growth rates of the primary producers in our model would require altering six parameters instead of the one (the community-level carrying capacity) that we alter in our simulations. However, ultimately the way in which environmental noise is implemented does not matter. Analyses of simple population models suggest that unless the population growth rate is extremely high, it does not make any difference in population dynamics whether environmental noise alters the carrying capacity or the growth rate (Mutshinda and O'Hara 2010). Our robustness analyses (Supplementary material Appendix 1) confirm this also in the case of our complex food web model, at least as long as the dynamics are close to the equilibrium (as was the case in our study).

The reddening with increasing trophic level reflects the buffering of the noise-induced population variability by complex food web dynamics such that the non-autocorrelated deterministic dynamics become positively autocorrelated (Fig. 3, 4), indicating increased similarity among population states between consecutive seasons. These observations are consistent among individual species of consumers, producers and fishes (Fig. 5, 6, Table 1, 2), suggesting that the patterns observed might reflect more generic properties of the food web dynamics rather than just the highly dominant impacts of certain guilds or species life-history stages.

Species' body size and trophic level, which are also closely correlated, explained some but not all of the reddening and dampening of the variation (Fig. 4, 5, Table 1, 2), implying that the pattern is not a straightforward function of the food web guild properties, but instead might be more related to the complex ways the species' positions and functioning interact

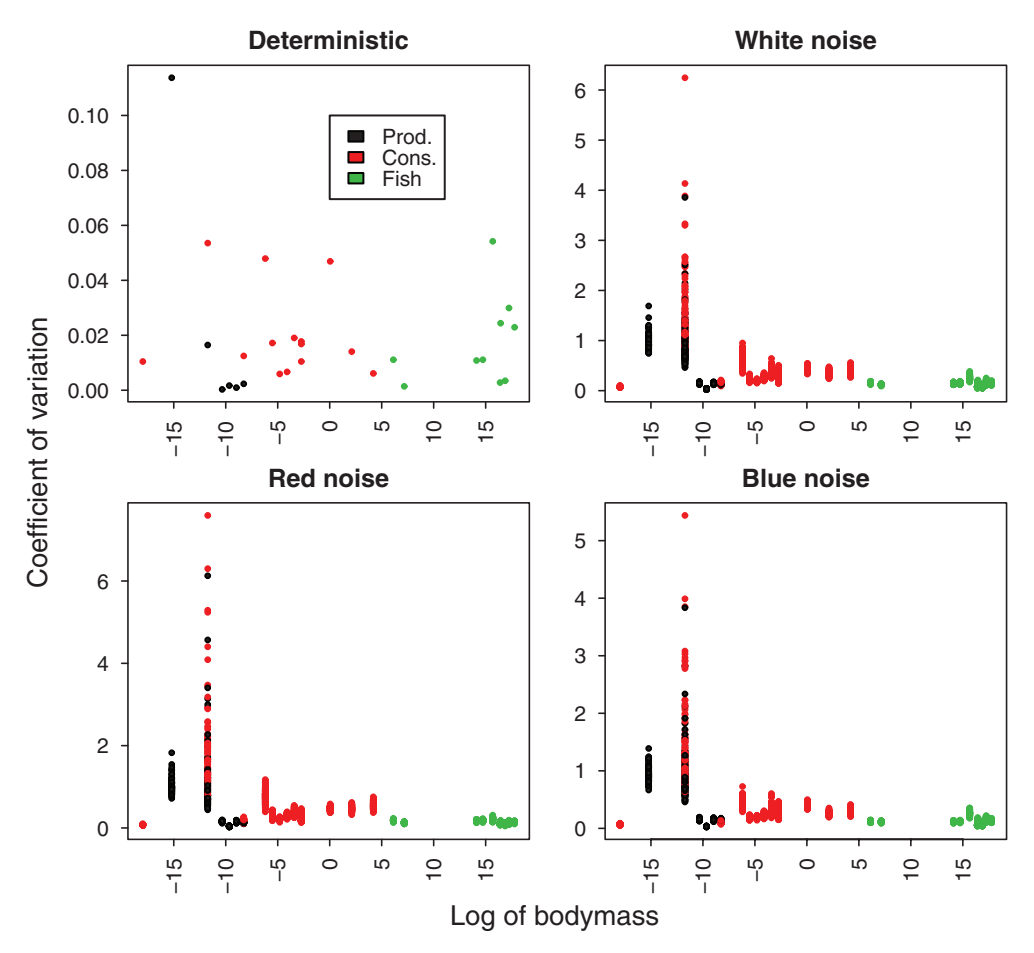


Figure 5. Coefficients of temporal biomass variation for each guild with respect to log-transformed body size of each guild. Individual points represent simulation runs across SD scenarios.

within the food web. Our research illuminates how abiotic variation may interact with complex ecological dynamics and provides a mechanistic and empirically realistic explanation why the observed fluctuations in ecological time series are often red irrespective of the colour of the environmental variables (Pimm and Redfearn 1988, Cohen 1995, Ripa et al. 1998). Whilst our analysis focussed on only one – albeit empirically well founded – aquatic food web, it sets the stage for the potential generalization of our results by studying a broader range of food webs. Such generality may be expected given the low reactivity of the predator—prey interaction networks to perturbations compared to mutualistic and competitive networks (Caravelli and Staniczenko 2016).

Most previous studies investigating the role of coloured environmental noise on species' dynamics have focussed on a single species and explored how environmental noise introduced into the demographic processes alters the fluctuations in the population dynamics (Kaitala et al. 1997, Reuman et al. 2008). These studies consistently find that the emerging fluctuations can be of any colour depending on the species' growth rates (Kaitala et al. 1997). A work more comparable to ours (Ripa et al. 1998) found that when coloured noise is introduced into the prey species abundance in a

two-species food web model, the variation in the predator population was generally redder than the variation in the prey population. Our current study demonstrates similar reddening of the variations as a result of the species' feeding interactions in a more complex, partly life-history structured food web, while at the same time emphasizing the need to explore the generality of this phenomenon using a larger set of modelled and empirically tested food webs and across alternative pathways through which the environmental noise is introduced into the food webs.

More recent work has explored these issues in models with more than one species. To the best of our knowledge, only the work of Lin and Sutherland (2013) has previously evaluated the effect of environmental noise and its colour on the dynamics of complex ecological networks. Contrary to our study, which incorporates environmental stochasticity only into the dynamics of the basal species of a single empirically well-parameterized food web, Lin and Sutherland introduce environmental stochasticity into the dynamics of all the species of hundreds of algorithmically-generated networks containing different types of species interactions (i.e. predation, parasitism and mutualism). The authors found that among several factors including the type of interspecific interactions,

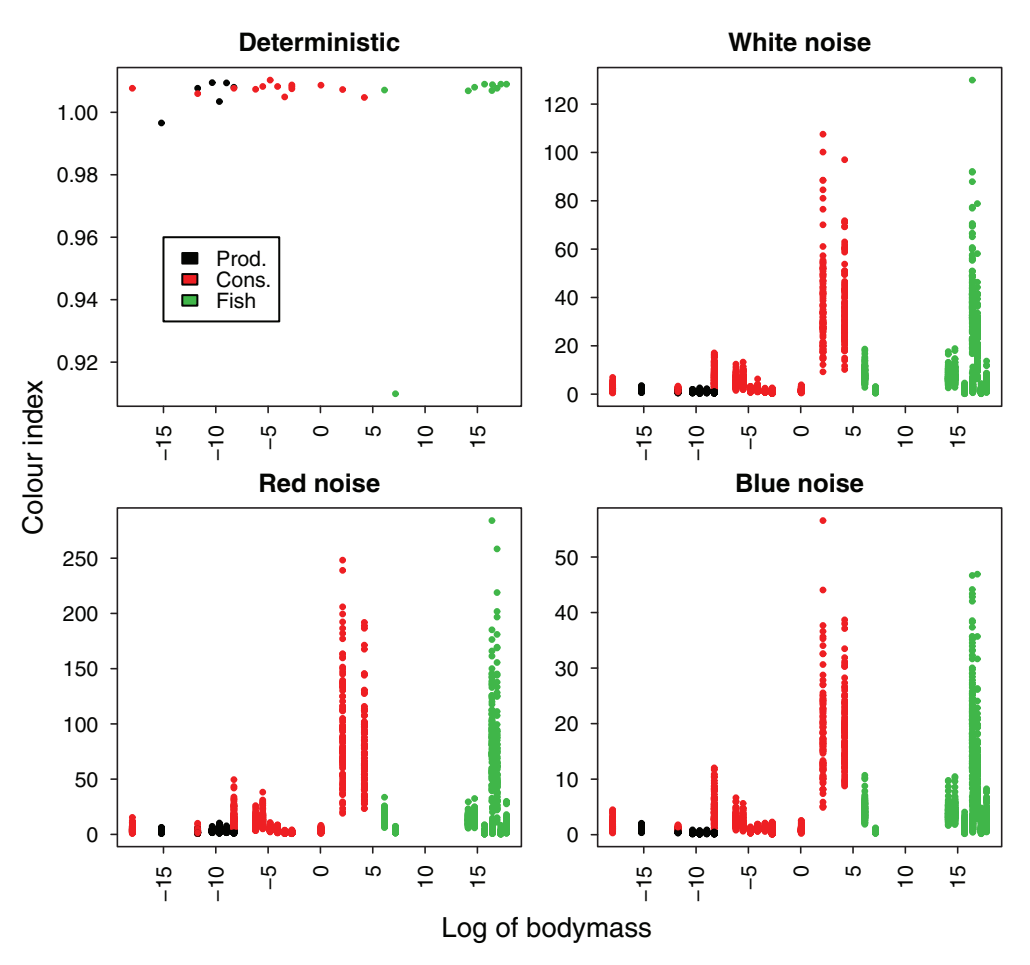


Figure 6. Colour indexes for temporal biomass variability with respect to log-transformed body size of each guild. Individual points represent simulation runs across SD scenarios.

both the synchrony of environmental noise across species and also the colour of the environmental noise explained most of the variation of the community dynamics. More specifically, white unsynchronized noise dampened and produced cycles in the population dynamics of the species within the networks, while red synchronized noise produced sudden outbreaks and crashes. The differences between this latter result and ours may be explained by their methodological choice of introducing the same stochasticity into every species in the network as well as forcing synchrony of the environmental noise across species. These two choices together most likely produce the dramatic oscillations experienced by their models with red noise (Lin and Sutherland 2013).

Historically, community ecologists have largely focused on how environmental fluctuations affect community structure and species coexistence (Chesson 1986). This focus has been mostly related to the long-standing debate of whether neutral (e.g. demographic stochasticity) or non-neutral (e.g. nichebased deterministic dynamics) processes determine the structure of ecological communities (Hutchinson 1961, Levins 1979, Chesson and Warner 1981, Loreau and Mazancourt 2008). In that context, Ruokolainen et al. (2009b) used a metacommunity approach to evaluate how different assembly

conditions such as environmental stochasticity, dispersal rate, and competition affect the similarity among local communities. The authors found that the environmental stochasticity introduced into the population dynamics of all species in each local community has no effect on the similarity of neutral communities in terms of species composition and abundance distributions. Likewise, white noise did not change the similarity of non-neutral communities, but red noise decreased the similarity of non-neutral communities. These results suggest that under the more realistic auto-correlated noise scenario, the structure of communities governed by deterministic competitive processes is less predictable than the structure of neutral communities. This contradicts our finding that a complex food web dampens the population fluctuations produced by red environmental noise, which suggests that non-neutral consumer-resource interactions within a community can increase the predictability of its structure (Berlow et al. 2009). However, the implicit assumption that the temporal similarity in our study is comparable to spatial similarity in studies of neutrality (Ruokolainen et al. 2009b) may be responsible for this discrepancy.

From an applied point of view, the present study provides important insights for environmental managers. Our

results illustrate how successive predator-prey interactions stabilize food webs by reducing both the magnitude and temporal variability of species. Increased reddening from the bottom to the top of the food web also implies increased predictability (positive autocorrelation) in the transient dynamics of the population (Caravelli and Staniczenko 2016) which, in the present study, emerge in response to yearly changes in the ecosystem productivity. This suggests that, besides maintaining single species of high conservation value, it is also important to maintain entire food webs including the long food chains on which such species depend. Likewise, our study emphasizes that multispecies modelling may more effectively elucidate how environmental noise affects population dynamics, whose colour may substantially affect the risk of extinction (Ripa and Lundberg 1996) among other population behaviours of much applied significance.

From a theoretical point of view, our network approach provides a powerful platform to build a theory able to predict the structure and dynamics of biological communities under environmental fluctuations. Future directions include exploring the effects of different network architectures (Williams and Martinez 2008), and interaction parameterizations such as those between parasites and hosts (Dunne et al. 2013) and between plants and their pollinators (Valdovinos et al. 2016). Generalities discovered through such exploration, such as, consistent changes in the colour with trophic level or interaction type (e.g. parasitism versus pollination) could be quantitatively tested against empirical data to determine the predictive ability of the theory. A theory that passes these tests could do much to elucidate the sensitivity of ecological systems to the profound changes in environmental variability currently being introduced into these systems.

Acknowledgements - We thank Jeff Hutchings and Stephanie Bland for inspiring discussions.

Funding – The research was funded by the Academy of Finland (AK), the Natural Sciences and Engineering Research Council of Canada (AK), European Research Council (COMPLEX-FISH 400820 to AK) and the USA National Science Foundation (DE SG0016247) and Department of Energy (ICER-1313830) (to NDM).

Statement of authorship – NDM and FSV share last authorship. AK and NDM conceived of the study. AK, TP and FSV designed the simulations. AK and TP developed the simulation code. Simulations were carried out by AK and TP. AK and TP developed the statistical and graphic analyses of the simulation outputs and conducted robustness analyses. AK, TP, FSV and NDM interpreted the results and wrote the manuscript.

References

- Berlow, E. L. et al. 2009. Simple prediction of interaction strengths in complex food webs. Proc. Natl Acad. Sci. USA 106: 187–191.
- Blarer, A. and Doebeli, M. 1996. In the red zone. Nature 380: 589–590.

- Boit, A. et al. 2012. Mechanistic theory and modeling of complex food web dynamics in Lake Constance. Ecol. Lett. 15: 594–602.
- Brose, U. et al. 2006. Consumer–resource body-size relationships in natural food webs. Ecology 7: 2411–2417.
- Burgers, G. 1999. The El Niño stochastic oscillator. Clim. Dynam. 15: 521–531.
- Caravelli, F. and Staniczenko, P. P. A. 2016. Bound on transient instability for complex ecosystems. – PLoS One 11: e0162430.
- Carscallen, W. M. A. et al. 2012. Estimating trophic position in marine and estuarine food webs. Ecosphere 3: 25.
- Ceballos, G. et al. 2017. Biological annihilation via the ongoing sixth mass extinction signaled by vertebrate population losses and declines. Proc. Natl Acad. Sci. USA 114: E6089–E6096.
- Chesson, P. L. 1986. Environmental variation and the coexistence of species. In: Diamond, J. and Case, T. (eds), Community ecology. Harper and Row, pp. 240–256.
- Chesson, P. and Kuang, J. J. 2008. The interaction between predation and competition. Nature 456: 235–238.
- Chesson, P. L. and Warner, R. R. 1981. Environmental variability promotes coexistence in lottery competitive systems. Am. Nat. 117: 923–943.
- Cohen, J. E. 1995. Unexpected dominance of high frequencies in chaotic nonlinear population models. Nature 378: 610–612.
- Dunne, J. A. et al. 2013. Parasites affect food web structure primarily through increased diversity and complexity. PLoS Biol. 11: e1001579.
- Halley, J. M. 1996. Ecology, evolution and 1/f-noise. Trends Ecol. Evol. 11: 33–37.
- Humphreys, W. F. 1979. Production and respiration in animal populations. J. Anim. Ecol. 48: 427–453.
- Hutchinson, G. E. 1961. The paradox of the plankton. Am. Nat. 95: 137–145.
- Kaitala, V. et al. 1997. Population dynamics and the colour of environmental noise. Proc. R. Soc. B 264: 943–948.
- Kuparinen, A. et al. 2016. Fishing-induced life-history changes degrade and destabilize fishery ecosystems. Sci. Rep. 6: 22245.
- Kuparinen, A. et al. 2018. Data from: environmentally-induced noise dampens and reddens with increasing trophic level in a complex food web. Dryad Digital Repository, http://dx.doi.org/10.5061/dryad.75mg6b1>.
- Levins, R. 1979. Coexistence in a variable environment. Am. Nat. 114: 765–783.
- Lin, Y. and Sutherland, W. J. 2013. Color and degree of interspecific synchrony of environmental noise affect the variability of complex ecological networks. – Ecol. Model. 263: 162–173.
- Loreau, M. and de Mazancourt, C. 2008. Species synchrony and its drivers: neutral and nonneutral community dynamics in fluctuating environments. Am. Nat. 172: E48–E66.
- Mougi, A. 2017. Persistence of age-structured food web. Sci. Rep. 7: 11055.
- Mutshinda, C. M. and O'Hara, R. B. 2010. On the setting of environmental noise and the performance of population dynamical models. BMC Ecol. 10: 7.
- Nielsen, M. V. and Olsen, Y. 1989. The dependence of the assimilation efficiency in *Daphnia* magna on the 14C-labeling period of the food algae *Scenedesmus acutus*. Limnol. Oceanogr. 34: 1311–1315.

- Pimm, S. L. and Redfearn, A. 1988. The variability of population densities. Nature 334: 613–614.
- Reuman, D. C. et al. 2008. Colour of environmental noise affects the nonlinear dynamics of cycling, stage-structured populations. Ecol. Lett. 11: 820–830.
- Ripa, J. and Lundberg, P. 1996. Noise colour and the risk of population extinctions. Proc. R. Soc. B 263: 1751–1753.
- Ripa, J. et al. 1998. A general theory of environmental noise in ecological food webs. Am. Nat. 151: 256–263.
- Ruokolainen, L. et al. 2009a. Ecological and evolutionary dynamics under coloured environmental variation. Trends Ecol. Evol. 24: 555–563.
- Ruokolainen, L. et al. 2009b. When can we distinguish between neutral and non-neutral processes in community dynamics under ecological drift? Ecol. Lett. 12: 909–919.

Supplementary material (available online as Appendix oik-05575 at <www.oikosjournal.org/appendix/oik-05575>). Appendix 1.

- Skalski, G. T. and Gilliam, J. F. 2001. Functional responses with predator interference: viable alternatives to the Holling type II model. Ecology 82: 3083–3092.
- Sugihara, G. 1995. From out of the blue. Nature 378: 559.
- Valdovinos, F. S. et al. 2016. Niche partitioning due to adaptive foraging reverses effects of nestedness and connectance on pollination network stability. – Ecol. Lett. 19: 1277–1286.
- Vasseur, D. A. and Yodzis, P. 2004. The colour of environmental noise. Ecology 85: 1146–1152.
- Walther, G.-R. et al. 2002. Ecological responses to recent climate change. Nature 416: 389–395.
- Williams, R. J. and Martinez, N. D. 2008. Success and its limits among structural models of complex food webs. J. Anim. Ecol. 77: 512–519.
- Yodzis, P. and Innes, S. 1992. Body size and consumer-resource dynamics. Am. Nat. 139: 1151-1175.